Quasi-two-body phase-space factors in the isobar model

Ramesh Bhandari
Center for Analysis of Particle Scattering, Department of Physics,
Virginia Polytechnic Institute and State University, Blacksburg, Virginia 24061
(Received 3 August 1981)

We present an integral representation of quasi-two-body phase-space factors in the isobar model, which is general enough to be used in phenomenological partial-wave scattering studies of systems such as πN, KN, NN, etc. We examine its analytic structure in detail, and furthermore cast it into an analytic form. This integral representation, with its analytic expression, is then convenient for use in analysis work.

I. INTRODUCTION

Within the framework of K and M ($\equiv K^{-1}$) matrix models, Bhandari *et al.*[1] recently discussed the existence of dibaryon resonances in the $^1D_2$ and the $^3F_3$ nucleon-nucleon partial waves. They employed a coupled-channel formalism, obtaining the elastic-scattering amplitude from the relation

$$T^{-1}=A-i\rho\ , \tag{1}$$

where T is a reduced-scattering-amplitude matrix in the channels involved. The product of its element T_{11} and ρ_e, the elastic phase-space factor, gives the conventional elastic partial-wave amplitude T_e. ρ_e and phase-space factors corresponding to the inelastic channels comprise the diagonal matrix ρ. Matrix A is the familiar K^{-1} or M matrix,[2] and in either case is free of threshold cuts. Because of this cut-free nature of matrix A, the T matrix in Eq. (1) clearly derives its right-hand unitarity cut structure from the ρ matrix.

The authors of Ref. 1 fitted the $^1D_2$ and the $^3F_3$ NN partial-wave phases of Arndt *et al.*,[3] using Eq. (1). These phases exist presently up to T_L (laboratory kinetic energy) $=800$ MeV and thus extend well beyond the pion-production threshold which is roughly at $T_L=300$ MeV. Under the assumption that the inelasticity in the above range of energy is mainly due to single-pion production which furthermore originates in the quasi-two-body channel $N\Delta$,[4] Eq. (1) is a 2×2 matrix equation, connecting channels NN and $N\Delta$. The inelastic phase-space factor corresponding to the channel $N\Delta$, which we denote by ρ_i, is then the only other diagonal element of the ρ matrix. In Ref. 1, the authors parametrized ρ_e as

$$\rho_e=[(s-s_e)/(s-c_e)]^{l_e+1/2}\ , \tag{2}$$

where s is the Mandelstam variable, equal to the square of the center-of-mass energy E. s_e is the elastic threshold energy squared, l_e is the orbital angular momentum in the elastic channel, and c_e is a parameter less than s_e. The numerator in ρ_e gives appropriate threshold behavior which includes centrifugal barrier effects. The denominator $(s-c_e)^{l_e+1/2}$, on the other hand, while giving a left-hand cut at c_e, provides modification of this behavior, such that as $s\to\infty$, $\rho_e\to 1$. Unlike ρ_e, the inelastic phase-space factor ρ_i must take into account the variable mass of the Δ isobar. Consequently, in Ref. 1, ρ_i appeared as the following integral:

$$\rho_i=\frac{1}{(E-c_i)^{l_i+1/2}}\int_{M_T=M_N+M_\pi}^{\infty}\frac{[E-(M_N+M)]^{l_i+1/2}(M-M_T)^{3/2}dM}{(M+\alpha)^{l_i+2}[(M-M_0)^2+\Gamma^2/4]}\ . \tag{3}$$

M_N and M_π are nucleon and pion masses, respectively. The complex mass of $\Delta=M_0-i\Gamma/2$. The factors in the numerator of the integrand represent the square-root threshold effects associated with the production of the Δ isobar with a relative orbital angular momentum of l_i, and its subsequent decay into N and π with a relative orbital angular momentum of 1 (see Fig. 1). The factor $(M+\alpha)^{l_i+2}$ in the denominator modifies the aforementioned threshold effects in the M depen-

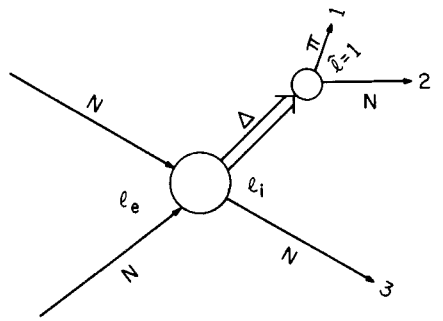

FIG. 1. Pion production via the isobar Δ in NN scattering. l_e, l_i, and $\hat{l}$ denote the relative orbital angular momenta for the systems NN, $N\Delta$, and πN, respectively.

dence, in the same sense as $(s-c_e)^{l_e+1/2}$ in the case of ρ_e. Its exponent l_i+2 is simply the sum of the exponents in the numerator of the integrand. The parameter α is real and greater than $-M_T$. The Breit-Wigner factor represents the isobar propagator of Fig. 1. The integral extends up to ∞, and is convergent. It has an imaginary part which accounts for the effect of the part of the continuous mass M, corresponding to $E<M+M_N$. Its complex nature is a consequence of the general analytic continuation procedure in which a two-body phase-space factor is replaced by i times its absolute value for energies below the corresponding threshold. The factor $(E-c_i)^{-(l_i+1/2)}$ outside the integral controls its behavior in the E variable. The parameter c_i is real and kept less than $s_e^{1/2}=M_N+M_N$. As in ρ_e, this factor also gives a left-hand cut which is at $E=c_i$ in this case.

Evidently, because of the coupling of the channels NN and $N\Delta$, the effect of $N\Delta$ production will be reflected in the elastic amplitude T_e, through the phase-space factor ρ_i. It thus becomes important to understand the analytic structure of ρ_i. The purpose of this paper is to extend the integral representation to the general case in which particles 1 and 2 are considered resonating with a relative orbital angular momentum $\hat{l}$, and to subsequently examine its form for analytic behavior. We discuss the integral for this general case in Sec. II. The integral can be easily cast into an analytic form, which we give in Appendix A. The availability of an analytic expression such as the one in Appendix A renders easy the phenomenological studies of partial-wave amplitudes for systems like the πN, KN, NN, etc. As mentioned earlier, Eq. (3) has already been used for the study of the energy dependence of the $^1D_2$ and the $^3F_3$ NN partial waves in Ref. 1.

II. ρ_i FOR THE GENERAL CASE, AND ITS ANALYTIC STRUCTURE

Generalizing Eq. (3) to the case in which particles 1 and 2, comprising the isobar, resonate with a relative orbital angular momentum $\hat{l}$, we write

$$\rho_i = f(E) g \Phi(E), \tag{4a}$$

$$g = \frac{\Gamma(M_0+\alpha)^{l_i+\hat{l}+1}}{2\pi(M_0-M_T)^{\hat{l}+1/2}}, \tag{4b}$$

$$\Phi(E) = \int_{M_T=M_1+M_2}^{\infty} \frac{(E-M_3-M)^{l_i+1/2}(M-M_T)^{\hat{l}+1/2}dM}{(M+\alpha)^{l_i+\hat{l}+1}[(M-M_0)^2+\Gamma^2/4]}, \tag{4c}$$

where particle 3 is the spectator produced in conjunction with the isobar of mass $M_0-i\Gamma/2$. The function $f(E)$ controls the behavior of $\Phi(E)$ away from the threshold. For example, in Eq. (3), it has a form which ensures that Re $\Phi(E)$ approaches a constant as $E\to\infty$. The normalization factor g is such that in the limit $\Gamma\to 0$, $g\Phi(E)\to(E-M_3-M_0)^{l_i+1/2}$.

A. Branch point at $E=E_T=M_T+M_3$

To determine the analytic behavior of $\Phi(E)$ in the immediate vicinity of the three-body threshold $E_T=M_3+M_T$ it is sufficient to consider only the square-root factors in Eq. (4c). Figure 2 shows the corresponding cuts in the complex M plane for $E<E_T$. There are two sheets attached to each one

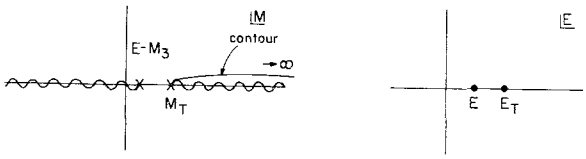

FIG. 2. The square-root branch points $E-M_3$ and M_T with their cuts for $E<E_T=M_T+M_3$. The contour of integration in the complex M plane extends to ∞.

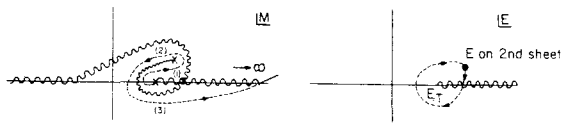

FIG. 4. Analytic continuation of $\Phi(E)$ to E on the second sheet of the cut at $E=E_T$ causes distortion of the contour of integration in the M plane.

of them. Each cut is present on both of the two sheets associated with the other. When $E<E_T$, it is clear that $\Phi(E)$ is single valued. But when E approaches E_T, the branch point at $M=E-M_3$ merges with the end point $M=M_T$ of the contour, suggesting that $E=E_T$ is a singularity.[5] Now, to continue beyond E_T, it is essential to assign a small imaginary part ϵ to E. If ϵ is positive, the analytic continuation takes place as shown in Fig. 3. The real part of $\Phi(E)$ is evidently positive. If, however, the analytic continuation is made beyond $E=E_T$ by assigning E a small negative imaginary part, Re $\Phi(E)$ is negative. On the other hand, the imaginary part of $\Phi(E)$, which corresponds to the part of the integral from $E-M_3$ to ∞, remains unaltered. These characteristics of $\Phi(E)$ imply a branch cut running from E_T to ∞ in the complex E plane, with discontinuity (from top to bottom) equal to 2 Re $\Phi(E)$. In addition, since $\Phi(E)$ is completely imaginary below E_T, $i\Phi(E)$ is a real analytic function.

Analytic continuation of the function $\Phi(E)$ in the E plane implies the movement of the branch point $E-M_3$ in the M plane. If in the process of analytic continuation, this branch point approaches the contour of integration, the contour must be distorted to avoid the branch point singularity from reaching it.[5] Consequently, a 2π rotation of the E vector around E_T in the E plane will cause the contour to be distorted in the manner shown in Fig. 4. When point E enters the unphysical sheet of the cut at $E=E_T$ in the E plane, the branch point $M=E-M_3$ in the M plane slips into the second sheet of the square-root cut at $M=M_T$,

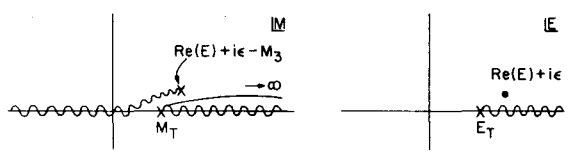

FIG. 3. Analytic continuation of $\Phi(E)$ to Re $(E)>E_T$ and Im $(E)=\epsilon>0$.

causing distortion of the contour. In the limit the imaginary part ϵ of E approaches zero, the segment (1) of the contour yields a value equal to Re $\Phi(E)$ of Fig. 3. This is due to the fact that in the evaluation of the integral for segment (1) in Fig. 4, both the vectors $M-M_T$ and $E-M_3-M$ are to be regarded as carrying an extra phase of -2π each due to the 2π rotation of E around $E=E_T$. Thus each of the square-root factors $(M-M_T)^{1/2}$ and $(E-M_3-M)^{1/2}$ has an extra negative sign which cancels the other since they enter as a product. The sign of $(E-M_3-M)^{1/2}$ on segment (2) is, however, positive since it lies on the other side of the cut. But this change in sign is offset by the negative sign that arises from the fact that integration is in the opposite direction, i.e., from $E-M_3$ to M_T. Thus the same value, namely, Re $\Phi(E)$, corresponding to the first sheet, obtains from segment (2). Segment (3), being close to the physical region and extending to ∞, yields the same contribution as the contour in Fig. 3. The contributions of these segments forming the entire distorted contour of Fig. 4 add up to give for E on the real axis of the second sheet of the cut at $E=E_T$,

$$\Phi(E)_{\text{IIsheet}}=3\,\text{Re}\,\Phi(E)+i\,\text{Im}\,\Phi(E)\ . \tag{5}$$

This result shows that the cut at $E=E_T$ cannot be of the simple square-root type. Rather, the further observation that subsequent 2π rotations of E around E_T in the same direction cause $\Phi(E)$ to increase at the rate of 2 Re $\Phi(E)$ per rotation suggests that the function must possess some kind of a logarithmic behavior at $E=E_T$ with an infinite number of sheets attached at that point [if we had chosen to make the aforementioned rotations in the opposite direction, we would have, instead, observed decreases in the real part of $\Phi(E)$ by the same amount]. Furthermore, from Eq. (4c), we find that Re $\Phi(E)$ in the vicinity of the threshold $E=E_T$ has the behavior

$$\mathrm{Re}\,\Phi(E)\approx\text{const}\int_{M_T}^{E-M_3}(E-M_3-M)^{l_i+1/2}(M-M_T)^{\hat{l}+1/2}dM=\text{const}\,B(l_i+\tfrac{3}{2},\hat{l}+\tfrac{3}{2})(E-E_T)^{l_i+\hat{l}+2}\,, \quad (6)$$

where $B(l_i+\frac{3}{2},\hat{l}+\frac{3}{2})$ is the familiar beta function (Euler's integral of the first kind).[6]

In view of the foregoing results, it is now possible to write for E near threshold,

$$\Phi(E)\sim(i/\pi)(E-E_T)^{l_i+\hat{l}+2}\ln(E_T-E)+i[a_0+a_1(E-E_T)+a_2(E-E_T)^2+\cdots]\,, \quad (7)$$

where a_k are real and a_0 is positive or negative according as l_i is even or odd.

B. Branch points at $E=E_\pm=M_0+M_3\pm i\Gamma/2$.

In the M plane, besides the two cuts already discussed, there are two complex conjugate poles at $M_\pm=M_0\pm i\Gamma/2$ and a pole of order $l_i+\hat{l}+1$ at $M=-\alpha$. These occur on all the sheets associated with the branch points at $M=M_T$ and $M=E-M_3$. Figure 5 shows separately the pinching of the contour between the branch-point singularity $E-M_3$ and the poles $M_0-i\Gamma/2$ and $M_0+i\Gamma/2$. These correspond, respectively, to analytic continuation of E to $E_-=M_0+M_3-i\Gamma/2$ and $E_+=M_0+M_3+i\Gamma/2$ on different nonprincipal sheets of the log cut (shown in Fig. 4), reached by burrowing through it from the top (for E_-) and the bottom (for E_+). Since pinching of a contour results in a singularity at that point,[5] the points $E=E_\pm$ are singular on these unphysical sheets. Figures 6 and 7 illustrate explicitly the singularity behavior of E_+. The contours in Fig. 7 are equivalent to the contours in Fig. 6. The contribution of the closed contour encircling the pole is of opposite sign in the two cases considered. In the first case, the closed contour integral yields

$$-2\pi i\times(\text{residue at } M_+=M_0+i\Gamma/2)=\frac{-2\pi}{\Gamma(M_++\alpha)^{l_i+\hat{l}+1}}(E-E_+)^{l_i+1/2}(M_+-M_T)^{\hat{l}+1/2}\,, \quad (8)$$

while in the second case the same expression obtains but with opposite sign, since the closed contour encircling the pole lies below the cut attached to $M=E-M_3$. Consequently, E_+ is a branch point with the discontinuity (top to bottom) across the associated cut (see Fig. 8) given by

$$D_+=\frac{4\pi}{\Gamma(M_++\alpha)^{l_i+\hat{l}+1}}(E-E_+)^{l_i+1/2}\times(M_+-M_T)^{\hat{l}+1/2}\,. \quad (9)$$

Likewise, the discontinuity across the cut, which also exists at $E=E_-$ (see Fig. 8), although on the different unphysical sheet, is

$$D_-=\frac{4\pi}{\Gamma(M_-+\alpha)^{l_i+\hat{l}+1}}(E-E_-)^{l_i+1/2}\times(M_--M_T)^{\hat{l}+1/2}\,. \quad (10)$$

The above cuts at E_+ and E_-, in fact, appear on all the nonprincipal sheets of the logarithmic cut at $E=E_T$, the discontinuity across them being different on different sheets. It is clear that E_+ and E_- are not singular on the principal sheet of the log cut because an analytic continuation to these points corresponds, in the M plane, to a direct movement of the branch point $E-M_3$ to the poles $M_0\pm i\Gamma/2$. That is, the point $E-M_3$ goes past the point M_T under it and over it (which is the reverse of what we have in Fig. 5) for analytic continuation to E_- and E_+, respectively, causing no distortion of the contour in either case.

In a similar fashion, we can show that branch points exist at $E=M_3-\alpha$ on all the unphysical sheets associated with the logarithmic cut. For suitable values of α, they can be made to lie to the left so as not to interfere with the right-hand cuts.

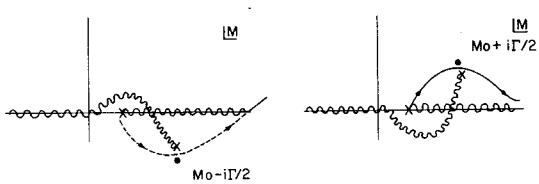

FIG. 5. Pinching of the contour between the branch point $E-M_3$ and the poles $M_0\pm i\Gamma/2$.

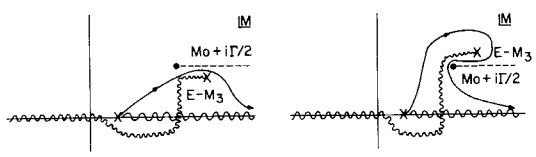

FIG. 6. Two possible ways of analytically continuing $\Phi(E)$ to E in the neighborhood of $E_+=M_0+M_3+i\Gamma/2$.

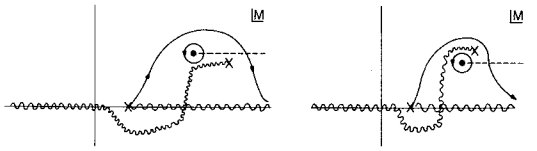

FIG. 7. The above contours are equivalent to the contours of Fig. 6 in the same order.

In Appendix A, we give the detailed analytic expression for $\Phi(E)$.

III. CONCLUSION

In summary, we have presented an integral representation for quasi-two-body phase-space factors which is general enough to be used in πN, KN, etc., partial-wave scattering studies. We have examined its analytic structure in detail and shown that the unitarity cut occurring in the partial-wave amplitude due to the onset of the three-body channel is of a logarithmic nature in contrast to the square-root nature of the two-body unitarity cut. Moreover, the enhanced strong interaction among two of the three particles in the final state, described by a Breit-Wigner propagator, gives rise to square-root cuts on the unphysical sheets attached to the three-body logarithmic cut. The standard procedure for analytic continuation easily yields discontinuities across these cuts. Furthermore, we are able to render the integral representation into a tractable, analytic form, convenient for use in the analysis. As pointed out earlier, we have already used it in the phenomenological study of the $^1D_2$ and the $^3F_3$ NN partial-wave amplitude.

ACKNOWLEDGMENTS

The author acknowledges useful conversations with Prof. R. E. Cutkosky. He also thanks Prof. R. A. Arndt for his comments. The Department of Energy supported this work.

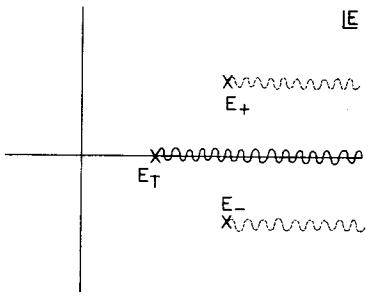

FIG. 8. The three-body logarithmic cut at $E=E_T=M_1+M_2+M_3$, and the quasi-two-body square-root cuts at complex-conjugate positions $E=E_\pm=M_0+M_3\pm i\Gamma/2$ on the unphysical sheets of the cut at $E=E_T$.

APPENDIX A

The integral

$$\Phi(E)=\int_{M_T}^{\infty}\frac{(E-M_3-M)^{l_i+1/2}(M-M_T)^{\hat{l}+1/2}dM}{(M+\alpha)^{l_i+\hat{l}+1}[(M-M_0)^2+\Gamma^2/4]}\,, \tag{A1}$$

after a series of substitutions, can be cast into the following form:

$$\Phi(E)=\frac{1}{2id^{l_i+1/2}}[I^{(1)}_{l_i,\hat{l}}-I^{(2)}_{l_i,\hat{l}}]\,, \tag{A2a}$$

where

$$I^{(j)}_{l_i,\hat{l}}(E)=\int_0^1\frac{(bz-a)^{l_i+1/2}(1-z)^{\hat{l}+1/2}dz}{z-z_j} \tag{A2b}$$

and

$$z_j=a/[c+(-1)^j id]\,, \tag{A2c}$$

$$a=M_T+\alpha,\quad b=E-M_3+\alpha\,,$$

$$c=\alpha+M_0,\quad d=\Gamma/2\,. \tag{A2d}$$

The integral $I^{(j)}_{l_i,\hat{l}}$ is further expressible as a sum of the series

$$I^{(j)}_{l_i,\hat{l}}=b\sum_{M=1}^{l_i}(bz_j-a)^{m-1}J_{l_i-m,\hat{l}}-(bz_j-a)^{l_i}\sum_{n=1}^{\hat{l}}(1-z_j)^{n-1}J_{0,\hat{l}-n}+(1-z_j)^{\hat{l}}I^{(j)}_{0,0}\,, \tag{A3}$$

where

$$J_{n_1,n_2}=\int_0^1(bz-a)^{n_1+1/2}(1-z)^{n_2+1/2}dz\,. \tag{A4}$$

The integrals J_{n_1,n_2} satisfy the recursion relations

$$J_{n_1,n_2}=\frac{(-1)^{n_1}ia^{n_1+3/2}}{(n_1+n_2+2)b}+\frac{(n_2+1/2)(b-a)}{(n_1+n_2+2)b}J_{n_1,n_2-1}\ , \tag{A5a}$$

$$J_{n_1,n_2}=\frac{(-1)^{n_1}ia^{n_1+1/2}}{n_1+n_2+2}+\frac{(n_2+1/2)(b-a)}{n_1+n_2+2}J_{n_1-1,n_2}\ . \tag{A5b}$$

Clearly, from $J_{0,0}$, J_{n_1,n_2} can be evaluated for all n_1 and n_2. Moreover, if $I^{(j)}_{0,0}$ is known, $I^{(j)}_{l_i,\hat{l}}$ can be determined. The phase-space factor $\Phi(E)$ which is obtained from $I^{(j)}_{l_i,\hat{l}}$, can thus be written as an analytic expression.

Straightforward integration by parts yields for $J_{0,0}$

$$J_{0,0}=i\left[\frac{a+b}{4b}\right]a^{1/2}+i\frac{(b-a)^2}{8b^{3/2}}\ln\left[\frac{a^{1/2}-b^{1/2}}{a^{1/2}+b^{1/2}}\right]\ . \tag{A6}$$

Similarly, the expression for $I^{(j)}_{0,0}$ is

$$I^{(j)}_{0,0}=-ia^{1/2}-i\frac{a+b-2bz_j}{2b^{1/2}}\ln\left[\frac{a^{1/2}+b^{1/2}}{a^{1/2}-b^{1/2}}\right]+i(a-bz_j)^{1/2}(1-z_j)^{1/2}\ln\left[\frac{(1-z_j)^{1/2}a^{1/2}+(a-bz_j)^{1/2}}{(1-z_j)^{1/2}a^{1/2}-(a-bz_j)^{1/2}}\right]\ . \tag{A7}$$

To determine the analytic structure of $\Phi(E)$, expressed in its analytic form, it is sufficient to consider $I^{(j)}_{0,0}$ and $J_{0,0}$. While $J_{0,0}$ has only a logarithmic branch point at $E=E_T$ (see Fig. 8), $I^{(j)}_{0,0}$ contains this branch point as well as the branch points at $E=E_\pm$ (see Fig. 8). By making appropriate expansions in Eqs. (A6) and (A7), it is now easy to verify the results Eqs. (6)–(9).

Threshold behavior for $l_i=0$, $\hat{l}=0$ is given by

$$\begin{aligned}\Phi=&\frac{ia}{(c-a)^2+d^2}\left[\frac{3\epsilon^2}{16a^2}-\frac{\epsilon^2}{8a^2}\ln 2+\frac{\epsilon^2}{8a^2}\ln(-\epsilon/2a)\cdots\right]\\&+\frac{1}{2d}\left\{\left[1-z_2-\frac{\epsilon z_2}{2a}\frac{\epsilon^2 z_2{}^2}{8a^2(1-z_2)}+\cdots\right]\ln\left[\frac{-z_2}{1-z_2}\right]\right.\\&\left.-\left[1-z_1-\frac{\epsilon z_1}{2a}-\frac{\epsilon^2 z_1{}^2}{8a^2(1-z_1)}+\cdots\right]\ln\left[\frac{-z_1}{1-z_1}\right]\right\},\end{aligned} \tag{A8}$$

where $\epsilon=E-E_T$. It is obvious that Φ is completely imaginary for $\epsilon<0$. For $\epsilon>0$, it has a real part which it acquires from the term

$$\frac{\epsilon^2}{8a^2}\ln\left[-\frac{\epsilon}{2a}\right]\underset{\epsilon>0}{\rightarrow}\frac{\epsilon^2}{8a^2}\ln\left[\frac{\epsilon}{2a}\right]-\frac{i\pi\epsilon^2}{8a^2}\ . \tag{A9}$$

In the above transformation, we have assumed that the analytic continuation is made to the top of the logarithmic cut as in Fig. 3. Inserting Eq. (A9) in Eq. (A8), we find

$$\mathrm{Re}\,\Phi\,|_{\text{threshold}(\epsilon>0)}=\frac{\pi\epsilon^2}{8a[(c-a)^2+d^2]}=\frac{\pi(E-E_T)^2}{8(M_T+\alpha)[(M_0-M_T)^2+\Gamma^2/4]} \tag{A10a}$$

which agrees with Eq. 6. Also from Eq. (A8), we find that at $\epsilon=0$, i.e., $E-E_T$,

$$\mathrm{Im}\Phi=\mathrm{Im}[(1-z_2)\ln\left[\frac{-z_2}{1-z_2}\right]]/d\ . \tag{A10b}$$

Behavior near $E=E_\pm=M_0+M_3\pm i\Gamma/2$. $E=E_\pm$ are branch points as noted in Sec. II and shown in Fig. 8. At $E=E_-$, $a-bz_1=0$ and the argument of the logarithmic function in the third term of $I^{(1)}_{0,0}$ reduces to

$$\gamma_1 = e^{i2\pi n}, \quad n = 0, \pm 1, \pm 2, \ldots . \tag{A11}$$

On the first sheet, $n=0$, and expansion of this logarithmic function around $E=E_-$ gives the result

$$i(a-bz_1)^{1/2}(1-z_1)^{1/2}\left[\frac{2(a-bz_1)^{1/2}}{(1-z_1)^{1/2}a^{1/2}} + \frac{\frac{2}{3}(a-bz_1)^{3/2}}{(1-z_1)^{3/2}a^{3/2}} + \cdots\right] \tag{A12}$$

for the third term in the expansion of $I^{(1)}_{0,0}$.

Clearly, there is no cut at $E=E_-$ on the I sheet. However, when $n\neq 0$, we immediately see that Eq. (A12) acquires an additional term, namely,

$$i2\pi n \times i(a-bz_1)^{1/2}(1-z_1)^{1/2} . \tag{A13}$$

Thus on the sheet characterized by integer n, there is a cut for which the discontinuity is given by

$$\text{discontinuity} = \left.\frac{2\pi i n \times 2i(a-bz_1)^{1/2}(1-z_1)^{1/2}}{2a^{1/2}id}\right|_{b=E_- -M_3+\epsilon_1+i\epsilon_2} \tag{A14a}$$

which upon substitution of b simplifies to

$$\frac{4}{\Gamma}\pi n \frac{(\epsilon_1+i\epsilon_2)^{1/2}}{(c-id)}(c-a-id)^{1/2} . \tag{A14b}$$

For $n=1$, which corresponds to the second sheet reached from the top of the logarithmic cut Eq. (A14b) reduces to Eq. (10).

---

[1]R. Bhandari *et al.*, Phys. Rev. Lett. 46, 1111 (1981).

[2]R. M. Dalitz and S. Tuan, Ann. Phys. (N.Y.) 10, 307 (1960); M. Ross and G. Shaw, *ibid.* 13, 147 (1961).

[3]R. A. Arndt, L. D. Roper, B. J. VerWest, Robert Clark, R. A. Bryan, and P. Signell, Virginia Polytechnic Institute and State University report (unpublished).

[4]S. Mandelstam, Proc. R. Soc. (London), A244, 491 (1958), D. V. Bugg, J. Phys. G 5, 1349 (1977).

[5]R. J. Eden *et al.*, *The Analytic S-Matrix* (Cambridge University Press, Cambridge, England, 1966), see Chap. 2.

[6]See, e.g., P. M. Morse and H. Feshbach, *Methods of Theoretical Physics* (McGraw-Hill, New York, 1953), Vols. I and II.